Molecular Crystals and Liquid Crystals

Publication details, including instructions for authors and subscription information:
http://www.tandfonline.com/loi/gmcl20

Guiding and Routing Light with Nematicons

Gaetano Assanto [a] & Marco Peccianti [a]

[a] NooEL - Nonlinear Optics and OptoElectronics Lab, Department of Electronic Engineering, INFN & CNISM, University "Roma Tre", Rome, Italy

Version of record first published: 22 Sep 2010

To cite this article: Gaetano Assanto & Marco Peccianti (2008): Guiding and Routing Light with Nematicons, Molecular Crystals and Liquid Crystals, 488:1, 163-178

To link to this article: http://dx.doi.org/10.1080/15421400802240540

Mol. Cryst. Liq. Cryst., Vol. 488, pp. 163–178, 2008

ISSN: 1542-1406 print/1563-5287 online
DOI: 10.1080/15421400802240540

Guiding and Routing Light with Nematicons

Gaetano Assanto and Marco Peccianti
NooEL – Nonlinear Optics and OptoElectronics Lab, Department of Electronic Engineering, INFN & CNISM, University "Roma Tre", Rome, Italy

We review the main properties and applications of Nematicons, spatial solitons in reorientational nematic liquid crystals, with emphasis on waveguiding and processing of optical information.

Keywords: liquid crystals; nematicons; nonlinear optics; reorientational response; signal routing; spatial solitons

I. INTRODUCTION

Liquid crystals in the nematic phase are characterized by a high degree of orientational order and a nearly zero degree of positional order. Thereby, their elongated or rod-like molecules, e.g., $\approx$3 nm in length and only $\approx$0.5 nm in diameter in the mixture E7, macroscopically form an effective uniaxial crystal with the optic axis along the major molecular axis or director $\mathbf{n}$ [1]. At optical frequencies the extraordinary refractive index $n_{\parallel}$ associated to an electric field $\mathbf{E}$ linearly-polarized along $\mathbf{n}$ is larger than its ordinary counterpart $n_{\perp}$ for fields $\mathbf{E} \perp \mathbf{n}$; hence, most nematic liquid crystals (NLC) are positive uniaxials. In the presence of an electric field their molecules tend to rotate in order to react to the torque $\mathbf{\Gamma} = 2\mathbf{D} \times \mathbf{E}$, with $\mathbf{D}$ the

We are grateful to C. Umeton, A. Dyadyusha, M. Kaczmarek, for making samples and expertise available, to I. C. Khoo and F. Simoni for enlightening discussions. Several PhD students and postdoctors have contributed to this work, including A. Alberucci, C. Conti, A. Fratalocchi, A. Pasquazi and A. Piccardi.

Present address: Marco Peccianti, Research Ctr. SMC INFM-CNR, P.le Aldo Moro, Rome, Italy.

Address correspondence to Gaetano Assanto, NooEL – Nonlinear Optics and Opto-Electronics Lab, Department of Electronic Engineering, Via della Vasca Navale 84, Rome 00146, Italy. E-mail: Assanto@uniroma3.it

electric displacement field, and so minimize the free energy density encompassing a distortion term $E_{\mathrm{d}} = 1/2\{K_1(\nabla\cdot\mathbf{n})^2 + K_2(\mathbf{n}\cdot\nabla\times\mathbf{n})^2 + K_3(\mathbf{n}\times(\nabla\times\mathbf{n})^2)\}$ and an interaction term $E_{\mathrm{int}} = -1/2(n_\parallel^2 - n)(\mathbf{n}\cdot\mathbf{E})^2$ due to $\mathbf{\Gamma}$, with K_i $(i = \mathrm{l}, 2, 3)$ the Frank elastic constants for splay, twist and bend, respectively. As the resulting rotation of the induced rod-like dipoles reduces the angle $(\pi/2 - \vartheta)$ between the director and $\mathbf{E}$ in the plane $(\boldsymbol{k}, \mathbf{n})$ associated to an extraordinary ("*e*") eigenwave, with $\boldsymbol{k}$ the wavevector, the *e*-refractive index increases according to the usual $n_e^2 = \left[\frac{\cos^2\vartheta}{n_\perp^2} + \frac{\sin^2\vartheta}{n_\parallel^2}\right]^{-1}$, being $\vartheta = \mathbf{n}\langle k$ (we neglected walk-off) [2–4]. The latter corresponds to a positive reorientational nonlinearity with $\Delta n = \Delta n_e|_\vartheta = 1/2\varepsilon_a n_e(\vartheta)\sin(2\vartheta)\Delta\vartheta$ and $\Delta\vartheta > 0$, i.e., the self-focusing type of response required to counterbalance beam diffraction and support self-confined light packets or optical spatial solitons [5–7]. Optical spatial solitons corresponding to an actual Δn are light-induced graded-index waveguides and offer the potential to draw reconfigurable photonic circuits without pre-realized guiding structures [8]; they have been observed in several media, with a large variety of nonlinear mechanisms [5,6,9]. In NLC, in particular, they can be stable in the two transverse dimensions owing to the saturating and nonlocal character of the material response: saturation is inherent to the angular molecular reorientation $\Delta\vartheta$ in the extraordinary principal plane, whereas nonlocality – i.e., a medium change even at some distance from an electro-magnetic perturbation – stems from the elastic forces between the molecules in the fluid, as modeled above by the constants K_i [l–4].

Owing to the self-focusing nonlinearity, modulational instability and spatial solitary waves have been widely investigated in NLC [10–15], including discrete solitons in one-dimensional waveguide arrays [16,17]. Optical spatial solitons in nematic liquid crystals, or *Nematicons*, are stable two-dimensional self-confined beams of light based on nonlinear molecular reorientation [18]. As the index perturbation able to counterbalance diffraction is substantially wider than the self-trapped beam, Nematicons belong to the class of highly-nonlocal or *accessible* solitons [19,20]: they form channel waveguides with a large numerical aperture and *breathe* in propagation, their transverse size oscillating as they propagate in a graded-index distribution [21]. Moreover, Nematicons are *robust* and can sense other Nematicons or perturbations even at some distance, i.e., they can survive the interaction with linear as well as nonlinear defects and experience long-range mutual attraction [10,22].

In this paper we review the most important features and applications of Nematicons, providing a simple model but deferring details

to more specialized publications. In Section II we describe the basic equation(s) and the first observations of Nematicons in Section III some of their main features. In Section IV we deal with electro-optic steering of spatial solitons in NLC by acting on an applied voltage, whereas in Section V we describe all-optical approaches for the deviation of Nematicons.

II. BASIC MODEL AND FEATURES

Let us consider a planar geometry such as the one sketched in Figure 1(a, d), with a glass cell containing an undoped NLC with a preset (voltage-induced) orientation of its director [23,24]. For an incoming beam linearly polarized along x (along the cell thickness) and propagating along z, the evolution of its slowly-varying envelope A can be described by:

$$2ik\frac{\partial A}{\partial z} + \nabla_{\perp}^2 A + k_0^2(n_{\parallel}^2 - n_{\perp}^2)\left[\sin(\vartheta)^2 - \sin(\vartheta_0)^2\right]A = 0 \qquad (1)$$

with k_0 the wavevector in vacuum, $k = k_0 \mathrm{n_e}(\vartheta)$, ϑ_0 the tilt of the NLC molecules in the absence of light and ϑ the overall angular orientation. Equation (1) is a "well-conditioned" nonlinear Schroedinger equation supporting stable solitary solutions owing to saturation. A preset distribution Θ in the absence of a beam is symmetric along x and determined by the externally applied (low-frequency) voltage $\mathrm{V} \approx \mathrm{h}E$, with h

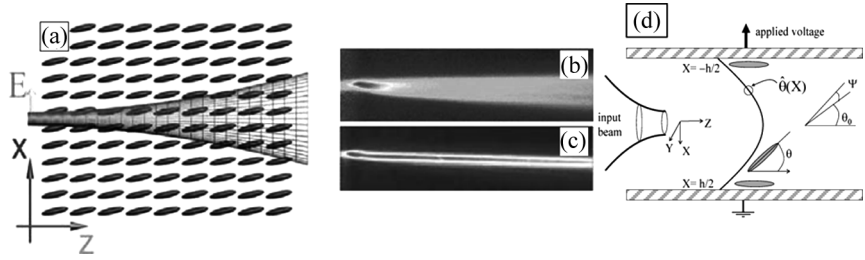

FIGURE 1 (a) A low-power optical beam with the electric field extraordinarily polarized in the x–z plane propagates forward in a sample with initial pre-tilt of the director. (b) Image of a 2 mW Argon-ion beam diffracting in a cell in the linear regime (polarized along y). (c) A spatial soliton generated be the same beam of panel (b) but in the nonlinear regime (polarized along x): a Nematicon propagates without spreading over a distance exceeding 1 mm (i.e., tens of Rayleigh lengths). (d) Sketch of the planar NLC cell. $\Theta(x)$ is the angle induced by the applied low-frequency voltage and $\theta_0 = \Theta(0)$. Ψ is the nonlinear perturbation. The cell can be considered invariant along y.

the cell thickness [24], according to

$$K\frac{d^2\Theta}{dx^2}+\frac{1}{2}\varepsilon_a E^2\sin(2\Theta)=0 \tag{2}$$

where K is the Frank constant taken equal for splay, bend and twist and ε_a the dielectric anisotropy in the quasi-static limit. The planar boundary conditions correspond to $\vartheta(x=-h/2)=\vartheta(x=h/2)\approx 0$. After setting $\vartheta(\mathrm{x},\mathrm{y},\mathrm{z})=\Theta(\mathrm{x})+\Theta/\vartheta_0\Psi(\mathrm{x},\mathrm{y},\mathrm{z})$ and $\Theta=\vartheta\cong\pi/4$ in order to maximize the reorientational response in a cell much thicker than the beam waist, we obtain

$$\begin{aligned} &2ik\frac{\partial A}{\partial z}+\nabla_\perp^2 A+k_0^2(n_\parallel^2-n_\perp^2)\Psi A=0\\ &4\pi K\nabla_{xyz}^2\Psi-8\nabla\varepsilon\Psi E^2+\pi\varepsilon_0(n_\parallel^2-n_\perp^2)|A|^2=0 \end{aligned} \tag{3}$$

System (3) includes a nonlocal correction to the standard Kerr model, and sustains stable and collapse-free propagation in nonlocal media. Introducing the free parameter α and normalized variables $\mathrm{A}=(\mathrm{A_c}/\alpha)a(\sqrt{x^2+y^2}/\mathrm{R_c}\sqrt{\alpha},\mathrm{z}/\mathrm{z_c}\alpha)\exp(\mathrm{z}/\mathrm{z_c}\alpha),\Psi=(\Psi_\mathrm{c}/\alpha/\Psi(\sqrt{x^2+y^2}/\mathrm{R_c}\sqrt{\alpha},\ \mathrm{z}/\mathrm{z_c}\alpha)$, with $\mathrm{A_c^2}=8\Delta\ \varepsilon\mathrm{E}^4/\pi\varepsilon_0 K k_0^2(n_\parallel^2-n_\perp^2)^2,\mathrm{z_c}=2k\mathrm{R_c^2},\ \mathrm{R_c^2}=\pi K/2\Delta\varepsilon\mathrm{E}^2,\Psi_\mathrm{c}=2\Delta\varepsilon\mathrm{E}^2/\pi K k_0^2(n_\parallel^2\ -n_\perp^2)^2$, solitons of Eq. (3) are described by

$$\nabla^2 a-a+\Psi a=0 \qquad \nabla^2\Psi-a\Psi+1/2a^2=0 \tag{4}$$

with a the envelope, Ψ the reorientational perturbation and α a figure of nonlocality able to describe solitons between the two limits: high nonlocality for small α and the (local) Kerr-case for infinite α [20]. The fundamental solitons of (4) are stable because realize an absolute minimum of the Hamiltonian [25]. Noteworthy, system (4) is formally equal to the set describing simultons in quadratic media with an electronic nonlinearity, where α would be the phase mismatch and Ψ the harmonic field [26]. In NLC, for comparable beam and reorientation profiles, local-type solitons (with large α) approximate well the solutions as the nonlinear perturbation is localized on-axis with respect to the excitation [27,28]. Conversely, in the small α limit – when the angular perturbation is much wider than the beam – the response is highly nonlocal. In the $\alpha\to 0$ regime, the soliton profile on-axis is Gaussian and depends on power rather than intensity, as expected from a highly nonlocal nonlinear response [13,19,20,29]. The latter model can be directly compared with our experiments: images were acquired with a CCD camera and a microscope taking advantage of the out-of-plane scattering, as shown in Figure 1(b–c) comparing the linear (diffraction) to the nonlinear outcome (Nematicon) [23]. Typical parameter values for the NLC mixture E7 at $\lambda=514\,\mathrm{nm}$ and in a

75 μm-thick cell biased at ≈1V are $(n_{\parallel}^2 - n_{\perp}^2) \approx 1$, $K \approx 10^{-11}$ N, E = 1.3 10^{-4} V/m, $\varepsilon_a \approx 20\varepsilon_0$ and $R_c = 22\,\mu m$. As powers ≤2 mW were launched into the cell, i.e., around 0.1 mW coupled inside the NLC, the highly nonlocal regime with $P \gg P_c = 16cn(\vartheta_0)\varepsilon_a E^2/k_0^2(n_{\parallel}^2 - n_{\perp}^2)^2 \approx 2\mu\ W$ was addressed, yielding a Nematicon waist of the order of 3 μm and a peak perturbation Ψ of about 10^{-3} (rad). The relationship between the Nematicon power P and its (intensity) waist W can be cast in the existence curve $PW^2 = P_c R_c{}^2$. When inputs do not exactly match (in power or waist) the stationary (z-independent) states on the existence curve, with $W \ll R_c$ or, equivalently, $P \gg P_c$, an arbitrary Gaussian input will in general excite a self-trapped oscillating beam or breather, with intensity and waist pulsating as it propagates and depending on the injected power [29].

III. SOME FUNDAMENTAL PROPERTIES OF NEMATICONS

Figure 2 shows some additional results enlightening the nonlocal nature of Nematicons. As pointed out above, the soliton waveguide has a numerical aperture larger than what strictly needed to guide the input light; hence, weaker copolarized signals of wavelength $>\lambda$ can also be confined in a Nematicon excited at λ [15,22]. This allows to transferring/transmitting signals of different wavelengths and modulation formats into Nematicons, paving the way to fully reconfigurable circuits for spatial multiplexing whereby the information can be routed in various directions or towards different output destinations by way of the light-induced channel(s) [30]. Noteworthy, owing

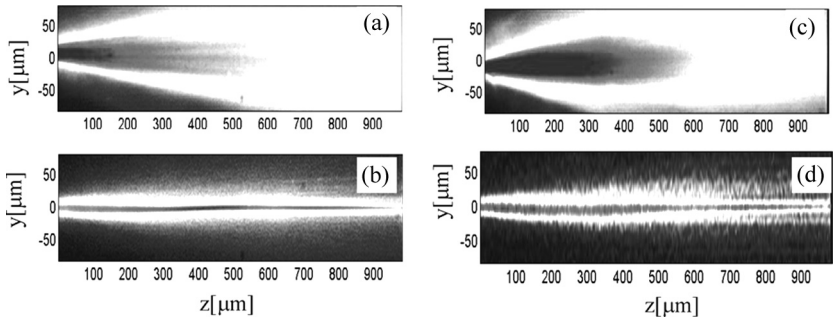

FIGURE 2 (a) y-polarized and (b) x-polarized 2.7 mW spatially incoherent (speckled) beam propagating at 514 nm in the NLC cell. A Nematicon forms in the extraordinary polarization where a reorientational response is driven. In (c) and (d) a 100 μW He – Ne incoherent signal is collinear and copolarized to the Argon beam in (a) and (b), respectively (tilt and offsets are artifacts).

to the spatial nonlocality, also a spatially (and/or temporally) incoherent, speckled (through a diffuser) beam can self-trap into a soliton if its power is large enough to overcome the higher diffraction (Fig. 2(a)) and form an "incoherent" Nematicon (Fig. 2(b)) [31–33]. Even in the incoherent case, the corresponding graded-index waveguide is such that a weak and copolarized signal propagating through the same diffuser follows the whereabouts of the stronger beam. In the example displayed in Figure 2, for instance, a naturally diffracting 100 μW He–Ne beam at 632.8 nm (Fig. 2(c)) becomes guided in the presence of a collinear copolarized spatially-incoherent Nematicon at 514 nm (Fig. 2(d)).

Since the NLC effectively is a uniaxial and Nematicons are extraordinarily polarized light packets, they undergo birefringent walk-off, i.e., their Poynting vector **S** (or photon flux) points in a slightly different direction than the wave vector $\boldsymbol{k}$. As in liquid crystals birefringence can easily be around 0.2 and reach 0.5, walk-off angles can be sizable. In E7 walk-off can be as large as 7°. In a cell such as in Figure 1(a, c), therefore, a Nematicon launched in the midplane $x = 0$ will move upwards/downwards along x despite its wavevector $\boldsymbol{k}//\boldsymbol{z}$. Eventually, the spatial soliton will approach the boundaries in $x = \pm h/2$ and interact with the refractive potential defined by the anchoring at the interfaces [34]. As a result, a Nematicon will follow a "snake-like" trajectory as it moves out-of-axis due to walkoff and feels the graded-index well in the cell (Fig. 3(a)). While such oscillations can be "tuned" by an applied voltage and exploited in the nonlinear regime to "correct" the soliton trajectory and output location (see Section V), they can be compensated by an initial tilt, as illustrated in Figure 3(b) [34]. Geometries with the director in the (y, z) plane, i.e. producing "side" steering (versus "depth") with respect to the plane of observation, have been exploited to control the Nematicon direction by varying the walkoff by an applied voltage, as we will address in Section IV. The plots in Figure 3 also emphasize the breathing nature of Nematicons, with cyclic changes in waist. Such breathing becomes rather involved when different wavelength components contribute to the formation of a spatial soliton via cross-phase modulation, as investigated by Alberucci and coworkers in the case of two-color nematicons [35].

Organic dopants (dyes) have been investigated in various NLC mixtures, as they can introduce optical absorption and gain in specific spectral intervals, at variance with undoped NLC which exhibit high transparency in a wide spectral range and a nonresonant nonlinearity [1]. Dye-doped NLC have been used to exploit the thermo-optic response through absorption, to enhance the nonlinearity through

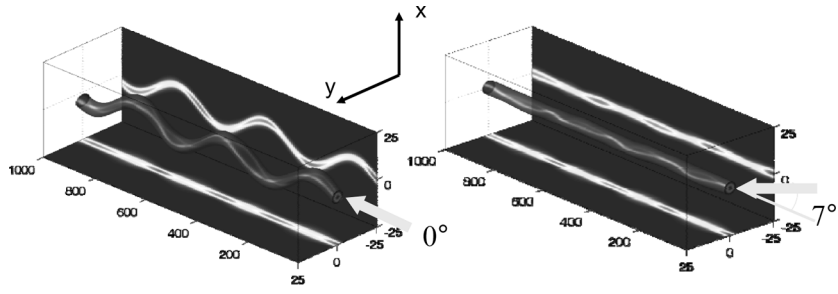

FIGURE 3 Typical trajectory of a Nematicon in a cell with molecules lying in the plane (x, z). (a) The input *e*-polarized beam is injected along z and forms a breather which interacts with the boundaries and propagates along an oscillatory path in (x, z). (b) The input beam is launched at an angle of 7° in order to compensate for the walkoff: as a result the Nematicon (still a breather) remains in the midplane.

the so called Janossy effect [36,37] and to produce light amplification and lasing action [38–40]. Noteworthy, the first evidence of beam self-focusing in liquid crystals was reported in dye-doped NLC by Braun and coworkers [41,42], and several experiments with solitary waves carried out in dye-doped systems using the temperature-mediated transition between nematic and isotropic phases [10,43,44]. In the reorientational regime, dye-doped NLC can sustain dissipative solitary waves, i.e., spatial solitons in the presence of absorption and/or amplification [45]. Dissipative Nematicons are characterized by breathing with aperiodic oscillations due to the varying power content.

IV. VOLTAGE CONTROLLED STEERING OF NEMATICONS

Nematic liquid crystals, reorientational molecular media with birefringent optical properties but in a fluid state, can be largely affected by the presence of a low-frequency or static electric field, i.e., an applied voltage [1,3]. An external bias, as outlined in Section I, can be used to eliminate the Freèdericks threshold and allow a continuous nonlinear response to an optical excitation, as exploited to produce low-power solitons [23]. The electro-optic response of NLC, however, can also be employed to modify their dielectric response, i.e., their birefringence and director orientation. While a change in birefringence will affect the nonlinear dynamics and degree of nonlocality [46,47], a reorientation in the optic axis can entirely redefine the principal axes and the extraordinary plane of the NLC uniaxial, thereby changing the

polarization state and the direction of propagation of a "walking" soliton beam [33]. An example is the application of an external bias to an NLC cell such as in Figure 1(d) or Figure 3: an electric field applied along x is able to modify the walkoff and the graded-index distribution and therefore alter the Nematicon oscillation in the plane (x, z).

Let us now consider the geometry sketched in Figure 4(a): planar anchoring with E7 director in the plane (y, z) at an angle $\rho \neq 0$, an *e*-polarized beam with electric field in (y, z) can generate a Nematicon. For e.g., $\rho = \pi/4$ with respect to z, the Poynting vector of such a Nematicon forms a walk-off angle $\approx 7^\circ$ with $\boldsymbol{k}//\boldsymbol{z}$. When a voltage V is applied across the cell thickness x, the electro-optic NLC response will drag **n** upwards and the *e*-plane out of (y, z), altering the director elevation ξ as well as the walkoff δ. As a result, the *apparent* walk-off of an *e*-wave, i.e., the direction of **S** as observed from above (y, z), will reduce with V until $\delta \approx 0^\circ$ when **n** is nearly parallel to **x**. Such steering is demonstrated by the photographs in Figure 4(b): the Nematicon launched at $V \approx 0\,V$ (i.e., below the Freèdericks threshold, top left panel), propagates at smaller and smaller angles with respect to z as V increases up to 2.1 V, when the director **n** is nearly //**x**. This agrees well with the calculated trend in Figure 4(c) (solid line), stemming from a plane-wave treatment and the material parameters of E7 [48]. Noteworthy, the wave packet forming a spatial solitons can effectively be treated as a plane wave despite its spectrum in space and conserve its polarization state despite the changes in optical anisotropy [49,50].

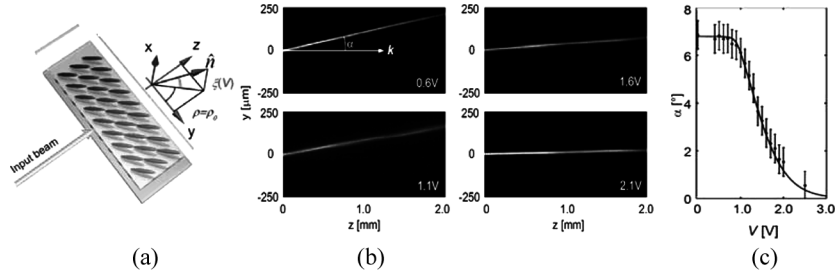

(a) (b) (c)

FIGURE 4 (a) Planar cell for birefringent routing in the plane (y, z): the director **n** forms an angle $\rho = \pi/4$ with respect to z at no bias, while the Poynting vector **S** to propagate at a walk-off of 7°. (b) Nematicon steering in (y, z) due to reduced apparent walk-off versus external voltage from 0.6 V (top left) to 2.1 V (bottom right). (c) Calculated and measured apparent walk-off versus voltage.

An angular deviation of 7 degrees is rather large for spatial solitons in optics; it could be made even larger by using NLC with higher birefringence. Nematicons, however, are robust and can survive the interaction with a discontinuity such as the transition to another transparent nonlinear medium supporting their propagation. It is therefore at hand the use of two distinct dielectric regions in order to exploit refraction through an interface. A simple cell structure can be designed similar to Figure 4(a) but with a top electrode split by a rectilinear gap in two portions 1 and 2, independently biased by different voltages (Fig. 5(a)) [51]. The index and birefringence mismatch between the two NLC regions below the electrodes can therefore be tuned in order to define the desired interface between the two nonlinear media and control the refraction of a Nematicon. When a soliton impinges on the (relatively narrow) gap separating the two dielectrics (1 and 2), the Nematicon can either be refracted or undergo total internal reflection (TIR), depending on the sign of the induced index mismatch as well as on the incidence angle below or above the corresponding critical value. Such phenomena in anisotropic dielectrics are not as simple as the usual Snell's law in isotropic media, but can be designed with the aid of the inverse surface of wave-normals [51]. Using a cell with planarly anchored director parallel to the gap, employing moderate voltages and near-infrared light at 1.064 μm in a cell with E7, for region 2 biased at higher voltage than region 1 we achieved refraction and angular steering of the self-induced waveguides up to -18°, as visible in Figure 5(b), center photo.

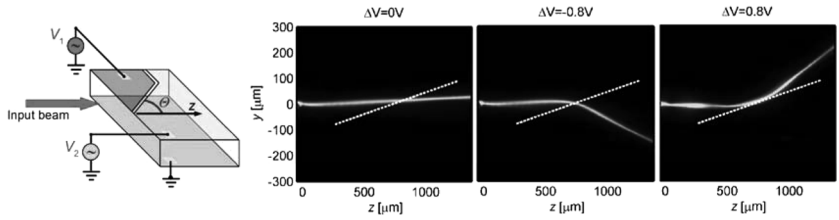

FIGURE 5 (a) Sketch of the NLC cell with two dielectric regions. On the top glass slide two electrodes are separated by a straight gap of 100 μm width (indicated by the white dashed line in (b)). Unequal voltages V_1 and V_2 applied to regions 1 and 2, respectively, induce different reorientations of the NLC molecules, i.e., distinct optical densities. (b) Intensity evolution of a 4.5 mW (input power) Nematicon along z. For $\Delta V = V_1 - V_2 = -0.8\,V \leq 0\,V$ the filament is refracted by -18° at the interface between regions 1 and 2. (b) When region 1 is optically denser than region 2, at $\Delta V = 0.8\,V$ and incidence above the critical angle, the Nematicon undergoes reflection with a deviation of 22°.

For region 1 biased with a higher voltage than region 2 and incidence angles $\geq 79^\circ$ we obtained total internal reflection refraction and a Nematicon deviation of $+22$ degrees, as shown in the rightmost panel of Figure 5(b). In this configuration and thanks to the peculiar anisotropy of NLC, optical solitons not only survive and maintain their extraordinary polarization, but also exhibit a large linear as well as a nonlinear Goos-Hänchen shift, with a corresponding power-controlled lateral displacement [52]. Finally, when the director is not parallel to the induced interface, the anisotropy allows non-specular (asymmetric) total internal reflection [53].

V. ALL-OPTICAL STEERING OF NEMATICONS

Since NLC are characterized by a large optical nonlinearity which supports Nematicons, the same all-optical reorientational response can be exploited in order to affect their propagation. Once again, the intrinsic robustness of these nonlocal solitons enables their non-destructive interaction with externally induced dielectric defects, other Nematicons, interfaces [21,50–57].

An all-optical defect can be created by employing a suitably polarized external beam in order to alter the refractive index and make a lens, as in Figure 6(a). Correspondingly, a Nematicon impinging on the lens-like perturbation will be either split into two branches or deviated sideways depending on its position relative to the defect, as

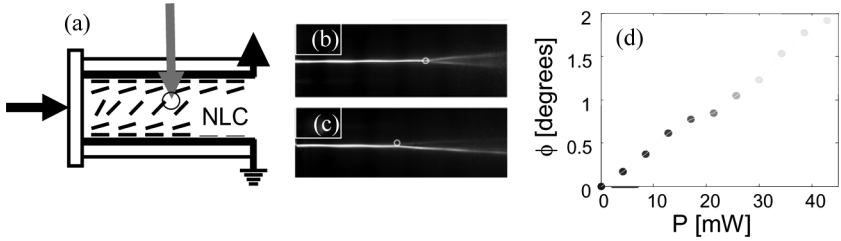

FIGURE 6 (a) Sketch of the geometry for inducing a defect by means of an external beam. The Nematicon is launched from left to right (E-field along x) and impinges on a lens-like defect as generated by the nonlinear NLC response to an external beam at 1.064 μm with E-field along z. (b–c) Effect of the perturbing beam of power P = 32 mW on the weak signal (He–Ne laser light at 0.6328 μm) guided by a Nematicon (at $\lambda = 1.064$ μm) in the (y, z) plane: (b) when the induced negative lens (its position marked by the circle) overlaps with the soliton, the confined beam splits up into a Y-junction; (c) as the lens is shifted upwards by $\Delta y = 9$ μm, the soliton and the signal are steered downwards; (d) plot of angular deviation in the case (c) versus input control power.

visible in the photographs taken at 1064 nm (Fig. 6(b–c)) [54]. The type of deviation and its size can be tuned by varying the power of the control beam (Fig. 6(d)), leading to potential all-optical gating and logic operations when employing more than one external inputs [55,56]. This approach to all-optical defects excited by external beam(s) can be generalized beyond the simple case of a lens, permitting the definition of various elements such as prisms or interfaces or periodic structures. An alternative to bulk-induced defects is the action of external light on the anchoring molecules at the boundaries, particularly in the presence of dyes [57].

While two high-power Nematicons intersecting at a wide angle behave as ideal Kerr solitons (see Fig. 7(a)), angular steering can also be obtained by the interaction of two or more of them in the plane (y, z) of propagation, provided their separation and relative angle are within the nonlocality range, as displayed in Figure 7(b–d) [22]. Owing to the high nonlocality of NLC, mutual Nematicon-Nematicon interactions, at variance with pure Kerr solitons, in most practical cases of interest

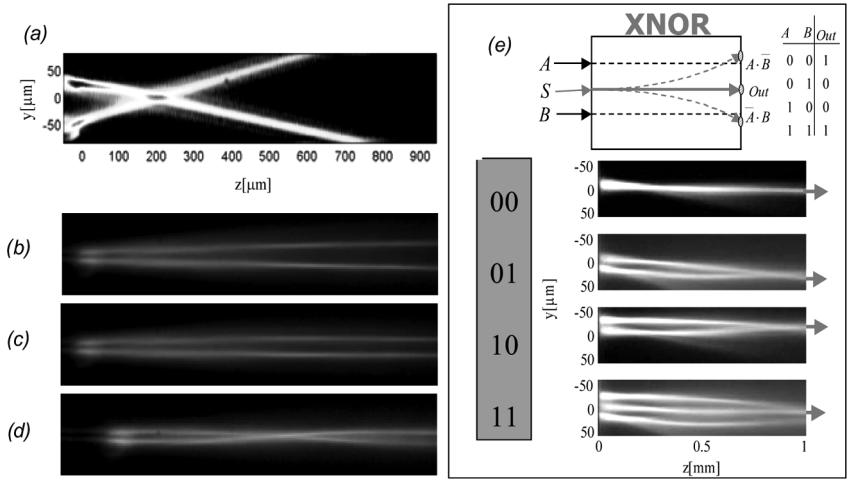

FIGURE 7 Nematicon interactions with another Nematicon. (a) Two high-power nematicons intersect at a wide angle, beahing as ideal solitons; (b) two low-power solitons (1.5 mW) launched at 514 nm (from the left side) with a relative angle of about 1.7°; (c) same as above, with a higher input power of nearly 2 mW each: the Nematicons propagate in parallel; (d) same as above with power >4 mW: interlacing and spatial switching of the outputs are clearly visible in the last case. (e) Example of an exclusive NOR logic gate with three Nematicons: A and B are control inputs, S carries the signal. The photographs show a demonstration with 1.7 mW Nematicons at 514 nm.

are attractive regardless the relative phase. If the degree of nonlocality can be lowered (e.g., by acting on bias) below a critical value, however, Nematicons attract/repel in the usual phase-dependent fashion characteristic of local solitons [58]. Two or more Nematicons can be arranged into all-optical logic gates, as the presence of a soliton can alter the path of the other(s) [59]. (Fig. 7(d) shows an exclusive NOR (XNOR) gate realized with two control soliton-inputs A and B, and a signal-carrying soliton S. The output of the latter at a given location (logic state TRUE) is altered by the presence (binary state 1) or the absence (binary state 0) of A and/or B, as summarized by the XNOR truth table.

While the interactions above took place in the plane (y, z), volume interactions can also occur. When two mutually attracting Nematicons are launched with initial tilts out-of-midplane, they can form a cluster with a finite angular momentum and spiral in propagation [60]. However, since the angular momentum of the system depends on the overall input power, clusters of high-power Nematicons will rotate faster than those with low-powers, leading to power-controlled rotation at the output [61]. Figure 8 shows an illustration of two spiraling Nematicons and the output image of the cluster as the input power is increased [62]. This phenomenon can be generalized to clusters of nematicons with different colours [63].

Several Nematicons, coherent or incoherent, [64–66] can be generated via transverse modulational instability, form clusters and undergo complex dynamics in both space and spectrum, [67,68] including the formation of optical shock waves in spite of the self-focusing nonlinearity [69,70].

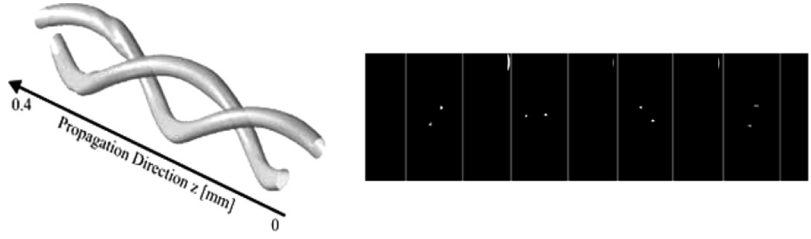

FIGURE 8 Nematicon interactions out of the plane (y, z). Left: sketch of spiraling Nematicons versus propagation. Right: images of the cluster in the output transverse plane (x, y) for various excitations: 2.1, 2.7, 3.3 and 3.9 mW in each beam, respectively. The boundaries of the NLC cell are indicated by vertical solid lines: as power increases, the cluster rotates faster, with a measured sensitivity of $\pi/2$ (rad)/mW.

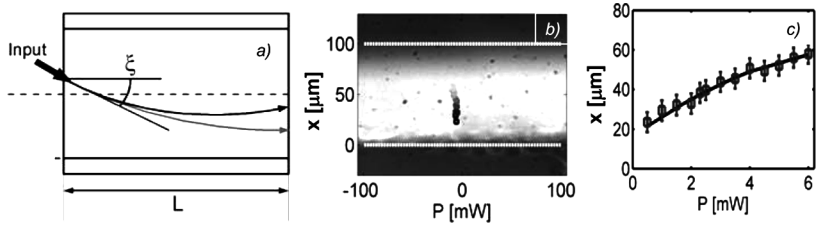

FIGURE 9 Power-dependent Nematicon bouncing at the boundary: (a) propagation and soliton trajectories in an NLC cell such as in Figure 1(c). Spatial solitons are launched with an elevation $\xi = 0.6^\circ$ in order to interact with the interface: as power increases, so does the repulsive force and the Nematicon is pushed away from the (lower) boundary (black line). (b) Acquired and superimposed photographs of Nematicon profiles at the cell output ($z = L = 4mm$) for various powers; the squares corresponding to the symbols in (c). (c) Experimental data (squares with error bars) and calculated (line) output soliton positions versus input power.

Finally, all-optical control on the propagation of a Nematicon can be gained by acting on its effective mass (power) as it interacts with the potential at the cell boundaries [71]. Since the nonlinear response is nonlocal and the potential gets altered by the soliton power, a simple way to displace a Nematicon consists in making it bounce off one of the boundaries: as the soliton power increases so does the repulsive force, pushing the self-trapped beam away as illustrated in Figure 9(a). Experimental results with Nematicons excited at 1.064 μm in a cell as in Figure 1(c) are shown in Figure 9(b–c) [72].

VI. CONCLUSIONS

In this brief (and incomplete) review on Nematicons we have tried to enlighten some of the most relevant features and recent results on spatial optical solitons in nematic liquid crystals. The experimental results, obtained with standard commercial NLC mixtures in simple planar cells, demonstrate the wealth of basic physics and potential applications of self-confined beams in these nonlocal dielectrics, making NLC an ideal workbench for soliton physics. Self-guiding and signal routing, angular steering and spatial multiplexing, electro-optic and all-optical control, switching, gating and polarization healing are just examples of the features encompassed by Nematicons and investigated to date. We anticipate several other phenomena and applications to be discovered and reported in the near future.

REFERENCES

[1] de Gennes, P. G. & Prost, J. (1993). *The Physics of Liquid Crystals*, Oxford U. Press: London, UK.
[2] Khoo, C. (1995). *Liquid Crystals: Physical Properties and Nonlinear Optical Phenomena*, Wiley: New York, USA.
[3] Tabyrian, N. V., Sukhov, A. V., & Zel'dovich, B. Ya. (1986). *Mol. Cryst. Liq. Cryst.*, *136*, 1.
[4] Simoni, F. (1997). *Nonlinear Optical Properties of Liquid Crystals and Polymer Dispersed Liquid Crystals*, World Scientific: Singapore.
[5] Stegeman, G. I., Christodoulides, D. N., & Segev, M. (2000). *IEEE J. Sel. Top. Quantum Electron.*, *6*, 1419.
[6] Kivshar, Y. S. & Agrawal, G. P. (2003). *Optical Solitons*, Academic Press: San Diego, USA.
[7] Conti, C. & Assanto, G. (2004). Nonlinear optics applications: Bright spatial solitons. In: *Encyclopedia of Modern Optics*, vol. 5, p. 43, Guenther, R. D., Steel, D. G., & Bayvel, L. (Eds.), Elsevier: Oxford, UK.
[8] Snyder, A. & Ladouceur, F. (1999). *Opt. Photon. News*, *10*, 35.
[9] Trillo, S. & Torruellas, W. (Eds.). (2001). *Spatial Solitons*, Springer-Verlag: Berlin, Germany.
[10] Warenghem, M., Henninot, J. F., Derrien, F., & Abbate, G. (2002). *Mol. Cryst. Liq. Cryst.*, *373*, 213.
[11] Henninot, J. F., Debailleul, M., & Warenghem, M. (2002). *Mol. Cryst. Liq. Cryst.*, *375*, 631.
[12] Assanto, G., Peccianti, M., Brzdąkiewicz, K. A., De Luca, A., & Umeton, C. (2003). *J. Nonl. Opt. Phys. Mat.*, *12*, 123.
[13] Peccianti, M., Conti, C., & Assanto, G. (2003). *Phys. Rev. E Rap. Comm.*, *68*, R025602.
[14] Karpierz, M. A., Sierakowski, M., Swillo, M., & Wolinsky, T. (1998). *Mol. Cryst. Liq. Cryst.*, *320*, 157; Karpierz, M. A. (2002). *Phys. Rev. E*, *66*, 036603.
[15] Hutsebaut, X., Cambournac, C., Haelterman, M., Adamski, A., & Neyts, K. (2004). *Opt. Commun.*, *233*, 211.
[16] Assanto, G., Fratalocchi, A., & Peccianti, M. (2007). *Opt. Express*, *15*, 5248.
[17] Lederer, F., Stegeman, G. I., Christodovlides, D. N., Assanto, G., Segev, M., & Silberberg, Y. (2008). *Phys. Rep., 463*, 1.
[18] Assanto, G., Peccianti, M., & Conti, C. (2003). *Opt. Photon. News*, *14*, 44.
[19] Snyder, A. W. & Mitchell, D. J. (1997). *Science*, *276*, 1538.
[20] Conti, C., Peccianti, M., & Assanto, G. (2003). *Phys. Rev. Lett.*, *91*, 073901.
[21] Peccianti, M., Conti, C., Assanto, G., De Luca, A., & Umeton, C. (2003). *J. Nonl. Opt. Phys. Mat.*, *12*, 525.
[22] Peccianti, M., Brzdąkiewicz, K. A., & Assanto, G. (2002). *Opt. Lett.*, *27*, 1460.
[23] Peccianti, M., Assanto, G., De Luca, A., Umeton, C., & Khoo, I. C. (2000). *Appl. Phys. Lett.*, *77*, 7.
[24] Assanto, G. & Peccianti, M. (2003). *IEEE J. Quantum Electron.*, *39*, 13.
[25] Turitsyn, S. K. (1985). *Theor. Math. Phys.*, *64*, 797.
[26] Assanto, G. & Stegeman, G. I. (2002). *Opt. Express*, *10*, 388.
[27] Garcia-Reimbert, C., Minzoni, A. A., & Smyth, N. F. (2006). *J. Opt. Soc. Am. B*, *23*, 294; Garcia-Reimbert, C., Minzoni, A. A., Smyth, N. F., & Worthy, A. L. (2006). *J. Opt. Soc. Am. B*, *23*, 2551.
[28] Minzoni, A. A., Smyth, N. F., and Worthy, A. L. (2007). *J. Opt. Soc. Am. B*, *24*, 1549.
[29] Conti, C., Peccianti, M., & Assanto, G. (2004). *Phys. Rev. Lett.*, *92*, 113902.

[30] Peccianti, M. & Assanto, G. (2001). *Opt. Lett.*, *26*, 1690.
[31] Peccianti, M. & Assanto, G. (2001). *Opt. Lett.*, *26*, 1791.
[32] Peccianti, M. & Assanto, G. (2002). *Phys. Rev. E Rapid Commun.*, *65*, 035603.
[33] Makris, K. G., Sarkissian, H., Christodoulides, D. N., & Assanto, G. (2005). *J. Opt. Soc. Am. B*, *22*, 1371.
[34] Peccianti, M., Fratalocchi, A., & Assanto, G. (2004). *Opt. Express*, *12*, 6524.
[35] Alberucci, A., Peccianti, M., Assanto, G., Dyadyusha, A., & Kaczmarek, M. (2006). *Phys. Rev. Lett.*, *97*, 153903.
[36] Janossy, I. & Lloyd, A. D. (1991). *Mol. Cryst. Liq. Cryst.*, *23*, 77.
[37] Janossy, I. (1994). *Phys. Rev. E*, *49*, 2957.
[38] Moreira, M. F., Carvalho, I. C. S., Cao, W., Bailey, C., Taheri, B., & Palffy-Muhoray, P. (2004). *Appl. Phys. Lett.*, *85*, 2691.
[39] Blinov, L. M., Cipparrone, G., Pagliusi, P., Lazarev, V. V., & Palto, S. P. (2006). *Appl. Phys. Lett.*, *89*, 031114.
[40] Blinov, L. M., Cipparrone, G., Mazzulla, A., Pagliusi, P., Lazarev, V. V., & Palto, S. P. (2007). *Appl. Phys. Lett.*, *90*, 131103.
[41] Braun, E., Faucheux, L., & Libchaber, A. (1993). *Phys. Rev. A*, *48*, 611.
[42] Braun, E., Faucheux, L., Libchaber, A., McLaughlin, D. W., Muraki, D. J., & Shelley, M. J. (1993). *Europhys. Lett.*, *23*, 239.
[43] Warenghem, M., Henninot, J. F., & Abbate, G. (1998). *Opt. Express*, *2*, 483.
[44] Derrien, F., Henninot, J. F., Warenghem, M., & Abbate, G. (2000). *J. Opt. A: Pure Appl. Opt.*, *2*, 332.
[45] Alberucci, A. & Assanto, G. (2007). *J. Nonl. Opt. Phys. Mat.*, *16*, 295.
[46] Peccianti, M., Conti, C., & Assanto, G. (2005). *Opt. Lett.*, *30*, 415.
[47] Conti, C., Peccianti, M., & Assanto, G. (2005). *Phys. Rev. E*, *72*, 066614.
[48] Peccianti, M., Conti, C., Assanto, G., De Luca, A., & Umeton, C. (2004). *Nature*, *432*, 733.
[49] Alberucci, A., Peccianti, M., Assanto, G., Coschignano, G., De Luca, A., & Umeton, C. (2005). *Opt. Lett.*, *30*, 1381.
[50] Assanto, G., Umeton, C., Peccianti, M., & Alberucci, A. (2006). *J. Nonl. Opt. Phys. Mat.*, *15*, 33.
[51] Peccianti, M., Dyadyusha, A., Kaczmarek, M., & Assanto, G. (2006). *Nature Phys.*, *2*, 737.
[52] Peccianti, M., Assanto, G., Dyadyusha, A., & Kaczmarek, M. (2007). *Opt. Lett.*, *32*, 271.
[53] Peccianti, M., Assanto, G., Dyadyusha, A., & Kaczmarek, M. (2007). *Phys. Rev. Lett.*, *98*, 113902.
[54] Pasquazi, A., Alberucci, A., Peccianti, M., & Assanto, G. (2005). *Appl. Phys. Lett.*, *87*, 261104.
[55] Serak, S. V., Tabiryan, N. V., Peccianti, M., & Assanto, G. (2006). *IEEE Photon. Techn. Lett.*, *18*, 1287.
[56] Assanto, G. & Peccianti, M. (2007). *J. Nonl. Opt. Phys. Mat.*, *16*, 37.
[57] Francescangeli, O., Lucchetti, L., Simoni, F., Stanić, V., & Mazzulla, A. (2005). *Phys. Rev. E*, *71*, 011702.
[58] Hu, W., Zhang, T., Guo, Q., Xuan, L., & Lan, S. (2006). *Appl. Phys. Lett.*, *89*, 071111.
[59] Peccianti, M., Conti, C., Assanto, G., De Luca, A., & Umeton, C. (2002). *Appl. Phys. Lett.*, *81*, 3335.
[60] Fratalocchi, A., Peccianti, M., Conti, C., & Assanto, G. (2004). *Mol. Cryst. Liq. Cryst.*, *421*, 197.

[61] Fratalocchi, A., Piccardi, A., Peccianti, M., & Assanto, G. (2007). *Opt. Lett.*, *32*, 1447.
[62] Fratalocchi, A., Piccardi, A., Peccianti, M., & Assanto, G. (2007). *Phys. Rev. A*, *75*, 063835.
[63] Assanto, G., Smyth, N. F., & Worthy, A. L. (2008). *Phys. Rev. A*, 78, 013832.
[64] Peccianti, M., Conti, C., & Assanto, G. (2003). *Opt. Lett.*, *28*, 2231.
[65] Assanto, G., Peccianti, M., & Conti, C. (2004). *IEEE J. Sel. Top. Quantum Electron.*, *10*, 862.
[66] Peccianti, M., Conti, C., Alberici, E., & Assanto, G. (2005). *Laser Phys. Lett.*, *2*, 25.
[67] Peccianti, M. & Assanto, G. (2005). *Opt. Express*, *13*, 6476.
[68] Peccianti, M. & Assanto, G. (2005). *Opt. Lett.*, *30*, 2290.
[69] Conti, C., Peccianti, M., & Assanto, G. (2006). *Opt. Lett.*, *31*, 2030.
[70] Ghofraniha, N., Conti, C., Ruocco, G., & Trillo, S. (2007). *Phys. Rev. Lett.*, *99*, 043903.
[71] Alberucci, A. & Assanto, G. (2007). *J. Opt. Soc. Am. B*, *24*, 2314.
[72] Alberucci, A., Peccianti, M., & Assanto, G. (2007). *Opt. Lett.*, *32*, 2795.